Nonreciprocal Polarization Converter Consisting of Asymmetric Waveguide With Magnetooptic Cladding: Theory and Simulation

Tomohiro Amemiya, *Student Member, IEEE*, Takuo Tanemura, *Member, IEEE*, and Yoshiaki Nakano, *Member, IEEE*

***Abstract*—A nonreciprocal polarization converter compatible with InP-based photonic integrated circuits is proposed. The device consists of an asymmetric InGaAsP waveguide combined with a ferrimagnetic cerium-substituted yttrium iron garnet layer. It makes use of the nonreciprocal conversion of the polarization state in the waveguide. A nonreciprocal TE–TM conversion efficiency of 93% at 1.55 μm wavelength can be obtained with a device length of 0.27 mm.**

***Index Terms*—Cerium-substituted yttrium iron garnet (Ce:YIG), finite-difference method (FDM) method, magnetooptical effect, photonic integrated circuits (PICs), polarization converter, waveguide optical isolator, III–V semiconductor.**

I. Introduction

AVOIDING the problems caused by undesired reflections of light is a matter of great importance in photonic integrated circuits (PICs). For this purpose, this paper proposes a waveguide-based nonreciprocal polarization converter that can be monolithically combined with other optoelectronic devices on a PIC.

A large-scale PIC incorporates a variety of waveguide-based optical devices integrated monolithically on an InP substrate to create desired optical functions in a single chip [1]–[3]. In such integration, connecting optical devices without the back reflection of light along a reverse direction is indispensable because the back reflection badly affects and destabilizes the operation of optical devices such as lasers and amplifiers. To cope with this problem, a lot of effort has been expended in developing waveguide-based isolators that can be integrated monolithically with other optical devices. Leading examples are the quasi-phase-matching (QPM) Faraday rotation isolator [4], [5], the nonreciprocal-phase-shift (NRPS) isolator [6], [7], and the nonreciprocal-loss (NRL) isolator [8]–[10]. They all make good use of nonreciprocal phenomena observed in a combination of semiconductor waveguides and magnetic materials. However, they are still in the experimental stage and have various problems. The QPM Faraday rotation isolator has yet to achieve a sufficient isolation ratio because of difficulty in making a large rotation of polarization; the NRPS isolator needs a large device length (>2 mm) and a complicated fabrication process because it uses a Mach–Zehnder interferometer; the NRL device has a large intrinsic loss caused by its operating principle, and therefore, needs a high-gain optical amplifier to reduce the insertion loss.

In this paper, we propose a novel unilateral device to prevent the detrimental effect of back reflected light in PICs. The device is a nonreciprocal TE–TM polarization converter that is compatible with InP-based PICs. It makes use of the magnetooptical transverse Kerr effect and the change in the state of polarization in an asymmetric semiconductor waveguide combined with a magnetic garnet. In most cases, disturbances caused by back reflection of light can be prevented simply by TE–TM polarization conversion because optical devices designed for use in one polarization is insensitive to the other. If necessary, we can make a waveguide isolator by attaching a waveguide polarizer to the nonreciprocal polarization converter (NRPC). The following sections first present the structure and the principle of our device, and then explain the method of electromagnetic analysis for the device. The operation of the device is confirmed by numerical calculation based on the finite-difference method (FDM). A nonreciprocal TE–TM conversion efficiency of 93% at 1.55-μm wavelength can be expected with a small device length of 0.27 mm.

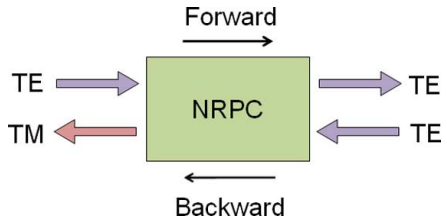

Fig. 1. Function of nonreciprocal polarization converter.

II. Device Structure and Operating Principle of NRPC

The basic function of NRPC is shown schematically in Fig. 1. Incident light with TE-mode passing through the NRPC in the forward direction maintains its TE mode and goes out from the right end of NRPC. In contrast, backward propagating TE-mode light is transformed into a TM mode in the NRPC and goes out from the left end. By inserting a NRPC at the output port of a laser, we can suppress the coherent interference between the lasing light and back-reflected light, which generally causes

Manuscript received August 30, 2008; revised November 08, 2008.

The authors are with the Research Center for Advanced Science and Technology (RCAST), University of Tokyo, Tokyo 153-8904, Japan (e-mail: ametomo@hotaka.t.u-tokyo.ac.jp; tanemura@hotaka.t.u-tokyo.ac.jp; nakano@ee.t.u-tokyo.ac.jp).

Color versions of one or more of the figures in this paper are available online at http://ieeexplore.ieee.org.

Digital Object Identifier 10.1109/JQE.2009.2013123

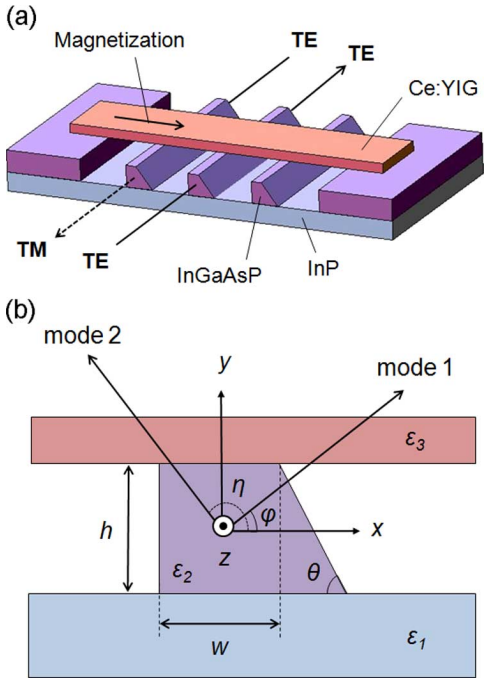

Fig. 2. Nonreciprocal polarization converters consisting of asymmetric InGaAsP waveguide with ferrimagnetic Ce:YIG. (a) 3-D view (three converters on an InP substrate are shown). (b) Cross-sectional view.

the instability of lasers. In addition, we can build a waveguide isolator by combining the NRPC with a waveguide polarizer or mode splitter [11], [12].

To create a waveguide NRPC compatible with InP-based PICs, we propose a device shown in Fig. 2(a). The NRPC device is formed on an InP substrate and consists of an asymmetric InGaAsP waveguide and a ferrimagnetic cerium-substituted yttrium iron garnet (Ce:YIG) layer attached on the top of the waveguide. The waveguide has a cross section with a right trapezoid shape, as shown in Fig. 2(b). The Ce:YIG layer is magnetized in the x-direction, and light travels in the z-direction. Process technology to form asymmetric waveguides [13]–[15] and wafer-bonding technology to attach garnet crystals to III–V semiconductor substrates [6], [16] have been established; this strongly supports the feasibility of our device.

To achieve polarization conversion, we make use of polarization rotation in the asymmetric waveguide. The orthogonal axes for eigenmodes in the asymmetric waveguide are rotated by φ with respect to the x–y axes, as shown by *mode 1* and *mode 2* in Fig. 2(b). The value of φ depends on the cross-sectional structure of the waveguide and can be set to 45° by optimizing the structure, as shown later. When $\varphi = 45°$, an incident TE-polarized light excites the two eigenmodes equally. Because of the difference in the propagation constant between mode 1 and mode 2, the state of polarization changes periodically as the light travels in the waveguide. The light is converted into a TM-polarized light after traveling the half-beat length. When the light travels one more half-beat length, it returns back to TE-polarized light. The half-beat length is given by

$$L_\pi = \frac{\pi}{|\beta_1 - \beta_2|} \tag{1}$$

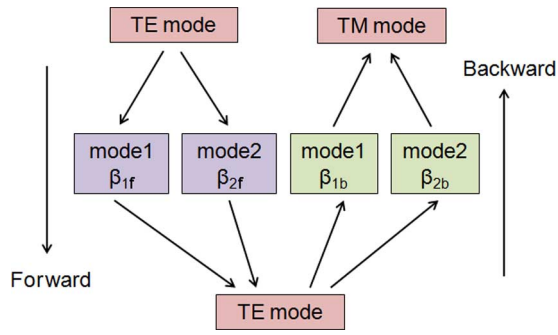

Fig. 3. Principle of nonreciprocal TE–TM conversion. Incident TE mode is resolved into two eigenmodes 1 and 2 with forward propagation constants β_{1f} and β_{2f}, and backward ones as β_{1b} and β_{2b}, then recombined into TE mode for forward propagation and into TM mode for backward propagation.

where β_1 and β_2 are the propagation constants of two eigenmodes, mode1 and mode 2. The values of β_1 and β_2 are different between forward and backward propagations because of the magnetooptic transverse Kerr effect induced by the Ce:YIG layer. Let us represent forward propagation constants by β_{1f} and β_{2f}, and backward ones by β_{1b} and β_{2b}. The necessary condition of our device is setting the half-beat length for backward propagation twice as large as that for forward propagation, i.e.

$$L = \frac{2\pi}{|\beta_{1f} - \beta_{2f}|} = \frac{\pi}{|\beta_{1b} - \beta_{2b}|}. \tag{2}$$

This condition can be satisfied by optimizing the device structure, as described in the next section. After traveling a distance of L, the two excited eigenmodes recombine into a TE mode for forward propagation and into a TM mode for backward propagation, as illustrated in Fig. 3. Therefore, the device with a length of L will operate as a nonreciprocal polarization converter.

In our NRPC device, only a small amount of propagating light interacts with the Ce:YIG layer because the refractive index of YIG is smaller than that of InGaAsP. However, as shown later, the magnetooptical Kerr effect induced by the Ce:YIG layer is large enough to make a sufficient difference in propagation constants to satisfy (2). Our device has two advantages over other waveguide isolators reported so far [4]–[10]. First, it can be smaller in length (<0.3 mm), which is described quantitatively through detailed analysis in the following sections. In addition, the device can be operated without external magnetic fields because the Ce:YIG normally has large remanence; this means that the device does not need electric power for operation.

The key to constructing our NRPC device is optimizing the waveguide structure so as to set $\varphi = 45°$ and satisfy (2). For this purpose, we performed electromagnetic calculation for the device operation. We first calculated the distribution of electromagnetic field only in the x–y plane to determine the optimized cross-sectional structure of the device, and then calculated the propagation pattern of light in the z-direction, using the vectorially corrected (VC) approach. The following sections describe the details of our analysis.

TABLE I
ALL THE PARAMETERS WE USED IN SIMULATION

Symbol	Parameter	Value
ε_1	Relative permittivity of InP substrate	$(3.16)^2$
ε_2	Relative permittivity of InGaAsP asymmetric waveguide layer	$(3.4)^2$
ε_3	Relative permittivity of Ce:YIG layer	$(2.2)^2$
Θ	Magneto-optical effect for Ce:YIG layer *	-4500 (deg/cm)
θ	Angle of the asymmetric waveguide †	53°
h	Height of the device	1.1 – 1.5 (μm)
w	Width of the device	0.9 – 1.4 (μm)

*This value has a great effect on off-diagonal elements of dielectric tensor for Ce:YIG.
†The angle is the same as that of InP $(1\,1\,1)$ plane.

III. DISTRIBUTION OF ELECTRIC FIELD IN THE CROSS SECTION

We first optimized the cross-sectional structure of our NRPC device with the aid of electromagnetic simulation in the x–y plane of the device. We used the FDM for the simulation.

The cross section of the device [see Fig. 2(b)] has three regions, i.e., an InP substrate, an InGaAsP ($\lambda_g = 1.25\ \mu$m) waveguide with a right trapezoid shape, and a ferrimagnetic Ce:YIG layer magnetized parallel to the x-axis. Let us represent the height and upper base length of the waveguide trapezoid by h and w. In simulations, we changed h from 1.1 to 1.5 μm and w from 0.9 to 1.4 μm. The wavelength of light was fixed to 1.55 μm. The refractive index was set to 3.16 for InP, 3.40 for InGaAsP, and 2.2 for Ce:YIG. The base angle θ of the waveguide trapezoid was set to 53° (angle for $(1\,1\,1)$ plane) because we assumed the trapezoid-shaped waveguide to be made using orientation-dependent chemical etching of InGaAsP $(1\,0\,0)$. We assumed that the InP substrate and the Ce:YIG layer were sufficiently thick in the computation domain. All the parameters we used are summarized in Table I.

Our device has the magnetized region, and therefore, we have to establish mathematical formulation for full-vector wave equations including the magnetooptical effect. The nonreciprocity is caused by the off-diagonal elements in the relative dielectric tensor of the Ce:YIG region. The relative dielectric tensor for each region in the device is given by

$$\varepsilon^{\mu\nu} = \begin{pmatrix} \varepsilon_r & 0 & 0 \\ 0 & \varepsilon_r & j\alpha \\ 0 & -j\alpha & \varepsilon_r \end{pmatrix} \tag{3}$$

where ε_r is the relative permittivity in each region. The off-diagonal element α is 0 except in the Ce:YIG. This element is related to the Faraday rotation coefficient Θ by equation $\alpha = 2n\Theta/k_0$, where k_0 is the wavenumber of light in vacuum and n is a refractive index (Θ in Ce:YIG is -4500 °/cm at a wavelength of 1.55 μm). We set the relative magnetic permeability of the garnet layer to 1 because macroscopic magnetization cannot follow a magnetic field at the frequency of light.

Using the relative dielectric tensors and Maxwell's equations, we obtained full-vector wave equations including the magnetooptical effect induced by the Ce:YIG. The equations are

$$\partial_x^2 E_x + \partial_y^2 E_x + \left(k_0^2\varepsilon_r - \beta^2\right)E_x + \partial_x\left(\frac{1}{\varepsilon_r}\partial_x\varepsilon_r E_x\right) + \partial_x\left(\frac{1}{\varepsilon_r}\partial_y\varepsilon_r E_y\right) + \alpha\omega\mu_0\partial_x\left(\frac{H_x}{\varepsilon_r}\right) = 0 \tag{4}$$

$$\partial_x^2 E_y + \partial_y^2 E_y + \left(k_0^2\varepsilon_r - \beta^2\right)E_y + \partial_y\left(\frac{1}{\varepsilon_r}\partial_x\varepsilon_r E_x\right) + \partial_y\left(\frac{1}{\varepsilon_r}\partial_y\varepsilon_r E_y\right) + \alpha\omega\mu_0\partial_y\left(\frac{H_x}{\varepsilon_r}\right) + jk_0^2\alpha E_z = 0 \tag{5}$$

where β is the propagation constant of light along the z-direction in the device, and E_i and H_i $(i = x, y, z)$ are electric field and magnetic field parallel to i-axis. In the InGaAsP waveguide and the InP substrate, the value of α is 0, so (4) and (5) are reduced to normal full-vector wave equations for transverse field components E_x and E_y. For the Ce:YIG region ($\alpha \neq 0$), we have to transform (4) and (5) into equations that involve only E_x and E_y. After laborious algebraic operations, we obtained the transformed equations

$$\partial_x^2 E_x + \partial_y^2 E_x + \left(k_0^2\varepsilon_r - \beta^2\right)E_x + \partial_x\left(\frac{1}{\varepsilon_r}\partial_x\varepsilon_r E_x\right) + \partial_x\left(\frac{1}{\varepsilon_r}\partial_y\varepsilon_r E_y\right) + \alpha\omega\mu_0\partial_x\left(\frac{\Psi}{\varepsilon_r}\right) = 0 \tag{6}$$

$$\partial_x^2 E_y + \partial_y^2 E_y - \beta^2 E_y + \Lambda + \partial_y\left(\frac{1}{\varepsilon_r}\partial_x\varepsilon_r E_x\right) + \partial_y\left(\frac{1}{\varepsilon_r}\partial_y\varepsilon_r E_y\right) + \alpha\omega\mu_0\partial_y\left(\frac{\Psi}{\varepsilon_r}\right) = 0 \tag{7}$$

where

$$\Psi = \frac{\alpha\omega\varepsilon_0}{\varepsilon_r\beta^2 + k_0^2\alpha^2}\left[\frac{\varepsilon_r\beta}{k_0^2\alpha}\left(\partial_x^2 E_y - \partial_x\partial_y E_x\right) - \partial_x(\varepsilon_r E_x) - \partial_y(\varepsilon_r E_y) - \frac{\varepsilon_r^2\beta}{\alpha}E_y\right] \tag{8}$$

$$\Lambda = \frac{k_0^2\alpha^2}{\varepsilon_r\beta^2 + k_0^2\alpha^2}\left(\partial_x^2 E_y - \partial_x\partial_y E_x\right) + \frac{\alpha\beta k_0^2}{\varepsilon_r\beta^2 + k_0^2\alpha^2} \times \left[\partial_x(\varepsilon_r E_x) + \partial_y(\varepsilon_r E_y) + \frac{\varepsilon_r^2\beta}{\alpha}E_y\right]. \tag{9}$$

Because of the nonzero off-diagonal element ($\alpha \neq 0$) in the Ce:YIG relative dielectric tensor, (6) and (7) involve linear terms in propagation constant β; this leads to a nonreciprocal solution to the propagation of light. The nonreciprocal solution gives a nonreciprocal polarization evolution (or a difference in the half-beat length between forward and backward propagations).

Equations for the InGaAsP and InP regions (i.e., (4) and (5) for $\alpha = 0$) and for the Ce:YIG region [(6)–(9)] can be solved with the aid of computer calculation based on the FDM. To solve these full-vector wave equations numerically, we partitioned the x–y plane into an 80×80 mesh with a mesh width (the difference between two adjacent space points) of 50 nm. Using the discrete form of the differential operators for normal full-vector wave equations (see [17] for these operators), we obtained finite-difference equations for the wave equations. We, then, solved these equations numerically to obtain forward- and backward-propagation constants for the two eigenmodes and the electric field components E_x and E_y. In our simulation, we assumed that the electric field showed an exponential attenuation outside the computational domain of 4×4 μm. We calculated

propagation constant β and electric fields $E_{\rm x}$ and $E_{\rm y}$ for various values of height h and base length w of the waveguide.

Using the results for β, $E_{\rm x}$, and $E_{\rm y}$, we calculated the effective index of refraction $(=\beta/k_0)$ in the waveguide for the two eigenmodes [mode 1 and mode 2 in Fig. 2(b)]. Fig. 4(a)–(c) shows the effective refractive index for forward and backward propagations, as a function of w, for different values of h. A significant difference between forward and backward propagation was observed only in mode 2. This is so because mode 2 has y-component $E_{\rm y}$ in its electric field in the Ce:YIG region, while mode 1 has not, as illustrated with Fig. 5(a-1) and (b-1). The nonreciprocity is produced by interaction between $E_{\rm y}$ and x-directed magnetization in the Ce:YIG. Theory and experimental results for this interaction have been reported in [6], [10], and [18]. In Fig. 5(a-1) and (b-1), length of arrows is not corresponding to field strength in order to make figures easy to see. Examples of actual calculated electric fields $E_{\rm x}$ and $E_{\rm y}$ for each mode are shown in Fig. 5(a-2), (a-3), (b-2), and (b-3).

Fig. 4(a)–(c) also shows that the difference in effective refractive index between forward and backward propagations increases with base length w and decreases with height h. The reason is as follows. A larger w increases the contact area between the waveguide and the Ce:YIG, and therefore, increases the magnetooptic interaction. In contrast, a larger h increases the distance between the Ce:YIG and the center of the distribution of light in the waveguide, and this decreases the magnetooptic interaction.

Using the results for electric fields, we calculated the half-beat length given by (1) and the rotation parameter R (see [19] for this parameter) defined by

$$R = \left| \frac{\int\int \varepsilon_r(x,y)\hat{E}_y(x,y)^2 dxdy}{\int\int \varepsilon_r(x,y)\hat{E}_x(x,y)^2 dxdy} \right| \tag{10}$$

for forward and backward propagations. In this equation, $E_x(x,y)$ and $E_y(x,y)$ are the x- and y-component of electric field at each mesh point (x,y), and $\varepsilon_r(x,y)$ is the diagonal element of the relative dielectric tensor at the point. Fig. 6(a)–(c) depicts the calculated values of the half-beat length and the rotation parameter as a function of w, for $h = (\mathrm{a})\ 1.1\,\mu\mathrm{m}, (\mathrm{b})\ 1.3\,\mu\mathrm{m}$, and $(\mathrm{c})\ 1.5\,\mu\mathrm{m}$. The rotation parameter R gives the angles φ and η (see Fig. 2) of eigenmodes as

$$|\varphi| = \left|\tan^{-1}(R)\right|, \qquad |\eta| = \left|\tan^{-1}\left(-\frac{1}{R}\right)\right|. \tag{11}$$

The efficiency of TE–TM conversion has a maximum at a distance of half-beat length, and the maximum value increases as R increases. A complete conversion can be obtained only when $R = 1$, i.e., angle φ should be 45°. The rotation parameter decreases as w and h increase. This is so because light is mainly distributed in the central part of the waveguide, and therefore, an increase in cross-sectional size of the waveguide decreases the asymmetry that light experiences during its propagation.

The necessary conditions for efficient nonreciprocal conversion are: 1) rotation parameter $R = 1$ to achieve a complete TE–TM conversion and 2) backward half-beat length is twice as large as forward one so as to satisfy (2). With the results of Fig. 6, we determined the optimal cross section structure of the waveguide to be $w = 1.0\ \mu$m and $h = 1.1\ \mu$m. In this simulation, smaller devices ($w < 0.9\ \mu$m, $h < 1.1\ \mu$m) were not

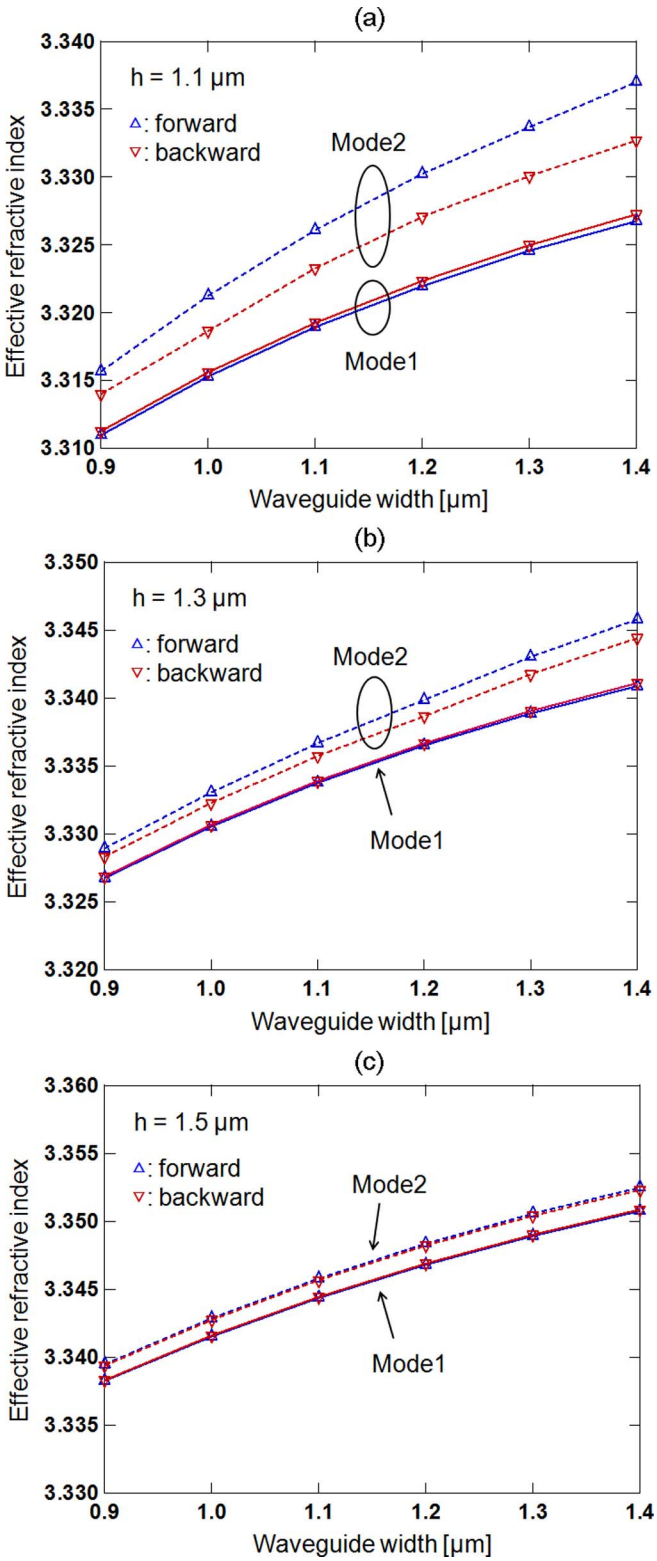

Fig. 4. Effective index of refraction in the waveguide for forward and backward propagations as a function of base length w, calculated for height $h = (\mathrm{a})\ 1.1\ \mu\mathrm{m}, (\mathrm{b})\ 1.3\ \mu\mathrm{m}$, and $(\mathrm{c})\ 1.5\ \mu\mathrm{m}$.

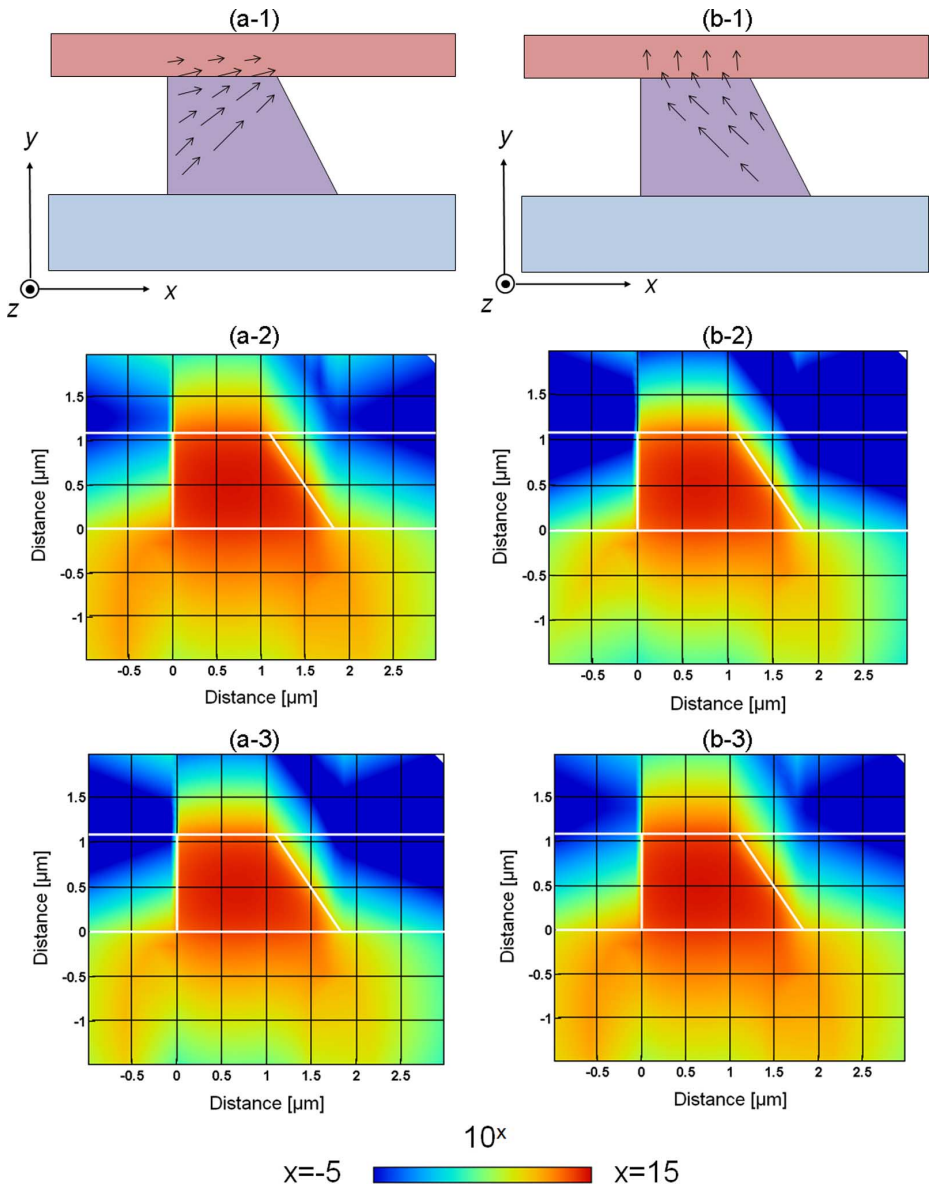

Fig. 5. Electric field distributions in the device. (a-1) and (b-1): direction of electric field, indicated by arrows for eigenmodes 1 and 2 (length of arrows is not corresponding to field strength in order to make figures easy to see). (a-2) and (b-2): $|\mathrm{E_x}|$ for eigenmodes 1 and 2. (a-3) and (b-3): $|\mathrm{E_y}|$ for eigenmodes 1 and 2. Parameters used are $\mathrm{w} = 1\ \mu\mathrm{m}$ and $\mathrm{h} = 1.1\ \mu\mathrm{m}$.

mentioned because they were not realistic when the limitation of the production technology was taken into consideration.

IV. Power Distribution of Light Along the Waveguide

Our next task is analyzing the propagation of light in the z-direction in a waveguide with the optimized cross section. For this purpose, we calculated the power distribution of light along the z axis as a function of propagation distance, using the VC approach [20]. In calculations, we assumed that the two orthogonal polarizations of eigenmodes in the waveguide took the following general form of

$$E_{x,y} = \psi(x,y) f_{x,y}(z) \exp(i\tilde{\beta} z) \tag{12}$$

where $f_x(z)$ and $f_y(z)$ are the amplitude of the transverse components E_x and E_y of electric field, and the parameter $\tilde{\beta}$ is a scalar propagation constant (see [21] and [22] for this expression). The scalar propagation constant $\tilde{\beta}$ can be related to the propagation constants β_1, β_2, and the rotation parameter R in our device. Here, let us represent the state of polarization $(= f_y(z)/f_x(z))$ by $u(z)$. In this section, we calculate the relation between $\tilde{\beta}$ and $\beta_1, \beta_2,$ and R. Then, we confirm the state of polarization $u(z)$ along z-axis.

Using Maxwell's equations with (3) and (12), we reached a differential equation that gives the evolution of $u(z)$ in the waveguide. The equation is

$$\partial_z u = \frac{i}{2\tilde{\beta}} D_{xy}(u + a_+)(u + a_-) \tag{13}$$

where

$$a_\pm = \frac{(D_{xx} - D_{yy})}{2D_{xy}} \pm \frac{\sqrt{(D_{yy} - D_{xx})^2 + 4D_{xy}D_{yx}}}{2D_{xy}}. \tag{14}$$

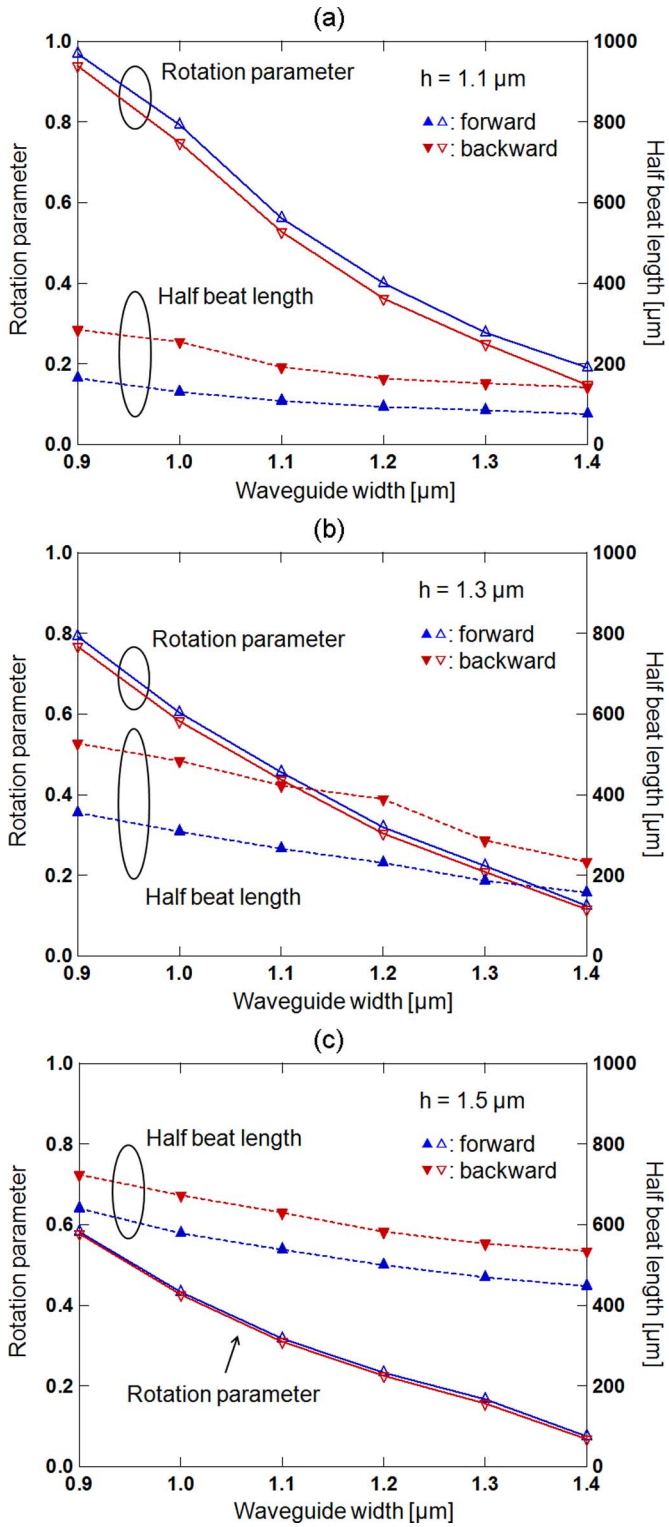

Fig. 6. Half-beat length and rotation parameter as a function of base length w, calculated for altitude h = (a) 1.1 μm, (b) 1.3 μm, and (c) 1.5 μm, at 1.55 μm wavelength.

Parameters D_{pq} ($p, q = x$ or y) in (14) are defined by the expression

$$D_{pq} = \frac{\int\int \psi \partial_p \psi \partial_q \left(\ln(\varepsilon_r) - (\alpha\tilde{\beta}/\varepsilon_r) \right) dxdy}{\int\int \psi^2 dxdy} \qquad (15)$$

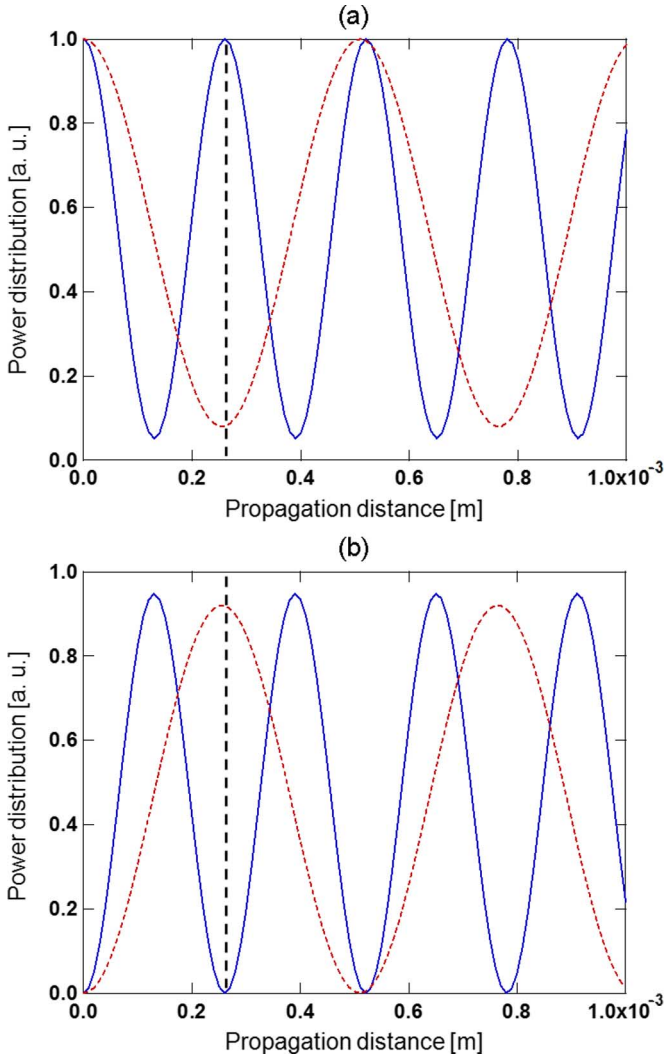

Fig. 7. Power distribution of light for a 1.55-μm TE-mode input, as a function of propagation distance. (a) TE component. (b) TM component, calculated for forward (solid curve) and backward (dashed curve) propagations. Maximum efficiency of conversion is obtained at propagation distance of 0.27 mm (dashed vertical line).

with a magnetooptical term of $(\alpha\tilde{\beta})/\varepsilon_r$. Because the direction of the optical axes corresponds to the direction in which a linearly polarized light propagating along z axis maintains its polarization state [i.e., $\partial_z u = 0$ in (13)]. Therefore, angles φ and η in Fig. 2(b) are given by

$$|\varphi| = \left|\tan^{-1}(a_+)\right|, \qquad |\eta| = \left|\tan^{-1}(a_-)\right|. \qquad (16)$$

Using (10), (11), and (16), we can rewrite $a_\pm$ as

$$a_+ = R = \frac{\int\int \varepsilon_r(x,y)\hat{E}_y(x,y)^2 dxdy}{\int\int \varepsilon_r(x,y)\hat{E}_x(x,y)^2 dxdy}$$
$$a_- = -\frac{1}{R} = -\frac{\int\int \varepsilon_r(x,y)\hat{E}_x(x,y)^2 dxdy}{\int\int \varepsilon_r(x,y)\hat{E}_y(x,y)^2 dxdy}. \qquad (17)$$

When TE-polarized light (polarized parallel to the x-direction) is given as an input at $z = 0$, its polarization state $u(z)$ ($u(0) = 0$) evolves with distance z and is given by

$$u(z) = \frac{1 - \exp\left(i(2\pi/L)z\right)}{a_+ - a_- \exp\left(i(2\pi/L)z\right)} \tag{18}$$

where

$$L = \frac{4\tilde{\beta}\pi}{|(a_+ - a_-)D_{xy}|}. \tag{19}$$

Parameter L is the linear beat length (twice as large as half-beat length), so it can be rewritten as $L = 2\pi/|\beta_1 - \beta_2|$ by using propagation constants $\beta_1 \text{and } \beta_2$ for the two eigenmodes. In consequence, the polarization state is given by

$$u(z) = \frac{1 - \exp\left(iz|\beta_1 - \beta_2|\right)}{a_+ - a_- \exp\left(iz|\beta_1 - \beta_2|\right)}. \tag{20}$$

Using (20), we calculated the power distribution of light along the z axis as a function of propagation distance. In calculations, we used the values of β_1 and β_2 obtained in Section III, and a_+ and a_- calculated using (17). Fig. 7 shows the results for an input of TE-polarized light, for forward (solid curve) and backward (dashed curve) propagations. Fig. 7(a) is the power distribution of the TE component of light, and Fig. 7(b) is that of the TM component. There is no TM components at $z = 0$ because we assume TE-polarized light as an input. As light travels in the waveguide, polarization conversion between TE and TM is repeated periodically. The period for backward propagation is twice as large as that for forward propagation, and this produces the nonreciprocal conversion. Forward-propagating TE-mode light returns to a TE mode after traveling 0.27 mm (the position indicated by a dashed vertical line), while backward-propagating TE-mode light is converted into TM mode after traveling the same distance. A nonreciprocal polarization conversion of 93% can be obtained with a device length of 0.27 mm. This way, we can construct waveguide NRPCs with high conversion efficiency.

V. Conclusion

We proposed a nonreciprocal TE–TM polarization converter that can be used to eliminate the disturbances caused by back reflection of light in InP-based PICs. Our device consists of an asymmetric InGaAsP waveguide combined with a ferrimagnetic Ce:YIG layer, making use of magnetooptical transverse Kerr effect and phase-mode mismatch in the waveguide. We described the guiding principle to design the optimal structure of the device. We also confirmed the operation of nonreciprocal TE–TM conversion by means of electromagnetic simulation. The results showed that a nonreciprocal conversion efficiency of 93% could be obtained with a device length of 0.27 mm at 1.55 μm wavelength. Our device can be upgraded to a waveguide isolator simply by combining with a polarizer or mode splitter. Our nonreciprocal polarization converter should be useful in integrating variety of optical devices on a photonic integrated circuit.

References

[1] T. L. Koch and U. Koren, "Semiconductor photonic integrated circuits," *IEEE J. Quantum Electron.*, vol. 27, no. 3, pp. 641–653, Mar. 1991.

[2] R. Nagarajan, C. H. Joyner, R. P. Schneider, Jr.,, J. S. Bostak, T. Butrie, A. G. Dentai, V. G. Dominic, P. W. Evans, M. Kato, M. Kauffman, D. J. H. Lambert, S. K. Mathis, A. Mathur, R. H. Miles, M. L. Mitchell, M. J. Missey, S. Murthy, A. C. Nilsson, F. H. Peters, S. C. Pennypacker, J. L. Pleumeekers, R. A. Salvatore, R. K. Schlenker, R. B. Taylor, H. S. Tsai, M. F. Van Leeuwen, J. Webjorn, M. Ziari, D. Perkins, J. Singh, S. G. Grubb, M. S. Reffle, D. G. Mehuys, F. A. Kish, and D. F. Welch, "Large-Scale photonic integrarted circuits," *IEEE J. Sel. Topics Quantum Electron.*, vol. 11, no. 1, pp. 50–65, Feb. 2005.

[3] J. W. Raring and L. A. Coldren, "40-Gb/s widely tunable transceivers," *IEEE J. Sel. Topics Quantum Electron.*, vol. 13, no. 1, pp. 3–14, Jan./Feb. 2007.

[4] B. M. Holmes and D. C. Hutchings, "Demonstration of quasi-phase-match nonreciprocal polarization rotation in III–V semiconductor waveguides incorporating magneto-optic upper claddings," *Appl. Phys. Lett.*, vol. 88, pp. 061116-1–061116-3, 2006.

[5] B. M. Holmes and D. C. Hutchings, "Towards the monolithically integrated optical isolator on a semiconductor laser chip," in *Proc. 19th Conf. IEEE Lasers Electro-Opt. Soc.*, Montreal, QC, 2006, pp. 897–898.

[6] H. Yokoi, T. Mizumoto, N. Shinjo, N. Futakuchi, and Y. Nakano, "Demonstration of an optical isolator with a semiconductor guiding layer that was obtained by use of a nonreciprocal phase shift," *Appl. Opt.*, vol. 39, no. 33, pp. 6158–6164, 2000.

[7] Y. Shoji and T. Mizumoto, "Wideband design of nonreciprocal phase shift magneto-optical isolators using phase adjustment in Mach–Zehnder interferometers," *Appl. Opt.*, vol. 45, no. 27, pp. 7144–7150, 2006.

[8] W. V. Parys, B. Moeyersoon, D. V. Thourhout, R. Baets, M. Vanwolleghem, B. Dagens, J. Decobert, O. L. Gouezigou, D. Make, R. Vanheertum, and L. Lagae, "Transverse magnetic mode nonreciprocal propagation in an amplifying AlGaInAs/InP optical waveguide isolator," *Appl. Phys. Lett.*, vol. 88, pp. 071115-1–071115-3, 2006.

[9] H. Shimizu and Y. Nakano, "Fabrication and characterization of an InGaAsp/InP active waveguide optical isolator with 14.7 dB/mm TE mode nonreciprocal attenuation," *J. Lightw. Technol.*, vol. 24, no. 1, pp. 38–43, Jan. 2006.

[10] T. Amemiya, H. Shimizu, P. N. Hai, M. Yokoyama, M. Tanaka, and Y. Nakano, "1.54-μm TM-mode waveguide optical isolator based on the nonreciprocal-loss phenomenon: Device design to reduce insertion loss," *Appl. Opt.*, vol. 46, no. 23, pp. 5784–5791, 2007.

[11] L. M. Augustin, R. Hanfoug, J. J. G. M. van der Tol, W. J. M. de Laat, and M. K. Smit, "A compact integrated polarization splitter/converter in InGaAsP-InP," *IEEE Photon. Technol. Lett.*, vol. 19, no. 17, pp. 1286–1288, Sep. 2007.

[12] L. M. Augustin, J. J. G. M. van der Tol, R. Hanfoug, W. J. M. de Laat, M. J. E. van de Moosdijk, P. W. L. van Dijk, Y. S. Oei, and M. K. Smit, "A single etch-step fabricatio n-tolerant polarization splitter," *J. Lightw. Technol.*, vol. 25, no. 3, pp. 740–746, Mar. 2007.

[13] H. El-Refaei, D. Yevick, and T. Jones, "Slanted-rib waveguide InGaAsP-InP polarization converters," *J. Lightw. Technol.*, vol. 22, no. 5, pp. 1352–1357, May 2004.

[14] J. Z. Huang, R. Scarmozzino, G. Nagy, M. J. Steel, and R. M. Osgood, Jr., "Realization of a compact and single-mode optical passive polarization converter," *IEEE Photon. Technol. Lett.*, vol. 12, no. 3, pp. 317–319, Mar. 2000.

[15] L. M. Augustin, J. J. G. M. van der Tol, E. J. Geluk, and M. K. Smit, "Short polarization converter optimized for active-passive integration in InGaAsP-InP," *IEEE Photon. Technol. Lett.*, vol. 19, no. 20, pp. 1673–1675, Oct. 2007.

[16] T. Mizumoto and H. Yokoi, "Waveguide optical isolators fabricated by wafer bonding," in *Proc. Mater. Res. Soc. Symp.*, 2005, vol. 834, pp. 135–146.

[17] W. P. Huang and C. L. Xu, "Simulation of three-dimensional optical waveguides by a full-vector beam propagation method," *IEEE J. Quantum Electron.*, vol. 29, no. 10, pp. 2639–2649, Oct. 1993.

[18] W. Zaets and K. Ando, "Optical waveguide isolator based on nonreciprocal loss/gain of amplifier covered by ferromagnetic layer," *IEEE Photon. Technol. Lett.*, vol. 11, no. 8, pp. 1012–1014, Aug. 1999.

[19] K. Saitoh and M. Koshiba, "Full-vectorial finite element beam propagation method with perfectly matched layers for anisotropic optical waveguides," *J. Lightw. Technol.*, vol. 19, no. 3, pp. 405–413, Mar. 2001.

[20] M. Fontaine, "Cross-phase modulation phenomena in strongly guiding waveguides: A theoretical approach revised," *J. Opt. Soc. Amer. B*, vol. 15, no. 3, pp. 964–971, 1998.

[21] H. G. Winful, "Self-induced polarization changes in birefringent optical fibers," *Appl. Phys. Lett.*, vol. 47, pp. 521–523, 1985.
[22] M. Fontaine, "Theoretical approach to investigating cross-phase modulation phenomena in waveguides with arbitrary cross sections," *J. Opt. Soc. Amer. B*, vol. 14, no. 6, pp. 1444–1452, 1997.

Tomohiro Amemiya (S'06) received the B.Sc. and M.Sc. degrees in electronic engineering in 2004 and 2006, respectively, from the University of Tokyo, Tokyo, Japan, and is currently working toward the Ph.D. degree in the Research Center for Advanced Science and Technology (RCAST), University of Tokyo.

From 2007, he was a Research Fellow in the Japan Society for the Promotion of Science (JSPS), Japan. His current research interests include physics of semiconductor light-controlling devices, optical spin-related devices, and in the processing technology to fabricate these devices.

He is a student member of the Optical Society of America and the Japan Society of Applied Physics. He was the recipient of the 2007 Laser Electro-Optical Society (LEOS, now the Photonics Society) Annual Student Paper Award and the 2008 IEEE LEOS Graduate Student Fellowships.

Takuo Tanemura (S'02–M'06) received the B.Sc., M.Sc., and Ph.D. degrees in electronic engineering from the University of Tokyo, Tokyo, Japan, in 2001, 2003, and 2006, respectively.

In 2006, he joined the Department of Electronic Engineering, the University of Tokyo, where he was in the Research Center for Advanced Science and Technology in 2007, where he is currently a Lecturer. His current research interests includes photonic-integrated circuits based on III–V semiconductors, photonic switching networks, and all-optical signal processing devices.

He is a member of the Institute of Electronics, Information and Communication Engineers of Japan. He was the recipient of the 2005 IEEE Laser Electro-Optical Society (now the Photonics Society) Graduate Student Fellowships and the Ericsson Young Scientist Award 2006.

Yoshiaki Nakano (S'81–M'87) received the B.E., M.S., and Ph.D. degrees in electronic engineering from the University of Tokyo, Tokyo, Japan, in 1982, 1984, and 1987, respectively. In 1984, he spent a year at the University of California, Berkeley, as an exchange student.

In 1987, he joined the Department of Electronic Engineering, University of Tokyo, where he was an Associate Professor in 1992, a Professor in 2000, and the Department Head in 2001, and is currently the Vice Director and a Professor in the Research Center for Advanced Science and Technology, and is also with the Department of Electronic Engineering, School of Engineering. In 1992, he was a visiting Associate Professor at the University of California, Santa Barbara. He was the Project Leader of the Japanese National Project on "Photonic Networking Technology" organized by the Ministry of Economy, Trading, and Industry, and as the Project Leader of the Solution Oriented Research for Science and Technology (SORST) Program on "Non-reciprocal Semiconductor Digital Photonic Integrated Circuits and their Applications to Photonic Networking" sponsored by the Japan Science and Technology Corporation. He authored and coauthored over 200 refereed journal publications and over 400 international conference papers, and holds 40 patents. He was the Editor-in-Chief of the *Applied Physics Express* (APEX) and *Japanese Journal of Applied Physics* (JJAP). His current research interests include physics and fabrication technologies of semiconductor distributed feedback lasers, semiconductor optical modulators/switches, and monolithically integrated photonic circuits.

Prof. Nakano was an elected member of the Board of Governors of the IEEE Laser Electro-Optical Society (LEOS, now the Photonics Society) and a member of the Board of Directors of the Japan Society of Applied Physics (JSAP). He is a member of the Board of Directors of the Japan Institute of Electronics Packaging (JIEP), the Chairman of the Optoelectronics Technology Trend Research Committee of the Optoelectronics Industry and Technology Development Association (OITDA), and the Chairman of the Optical Interconnect Standardization Committee of Japan Electronics Packaging and Circuits Association. He is also a Fellow of the Institute of Electronics, Information, and Communication Engineers (IEICE) and a member of the IEEE Electron Devices Society and the Optical Society of America. He is the recipient of the 1987 Shinohara Memorial Prize from the IEICE, the 1991 Optics Paper Award from the JSAP, the 1997 Marubun Science Prize, the 2007 Ichimura Prize, the 2007 IEICE Electronics Society Award, and the 2007 Sakurai Medal from the OITDA. He was presented the Prime Minister Award in Collaborative Research between Academia and Industry in 2007.